Published in final edited form as:
Biomaterials. 2013 October ; 34(31): 7584–7591. doi:10.1016/j.biomaterials.2013.06.036.

The use of plasma-activated covalent attachment of early domains of tropoelastin to enhance vascular compatibility of surfaces

Matti A. Hiob[a,b], **Steven G. Wise**[b,a], **Alexey Kondyurin**[c], **Anna Waterhouse**[d], **Marcela M. Bilek**[c,#], **Martin K. C. Ng**[b,e,#], and **Anthony S. Weiss**[a,f,g,#,*]

[a]School of Molecular Bioscience, University of Sydney, NSW 2006, Australia

[b]The Heart Research Institute, Sydney, NSW 2042, Australia

[c]School of Physics, University of Sydney, NSW 2006, Australia

[d]Wyss Institute for Biologically Inspired Engineering, Harvard, Boston, MA 02115, USA

[e]Department of Cardiology, Royal Prince Alfred Hospital, NSW 2050, Australia

[f]Bosch Institute, University of Sydney, NSW 2006, Australia

[g]Charles Perkins Centre, University of Sydney, NSW 2006, Australia

Abstract

All current metallic vascular prostheses, including stents, exhibit suboptimal biocompatibility. Improving the re-endothelialization and reducing the thrombogenicity of these devices would substantially improve their clinical efficacy. Tropoelastin (TE), the soluble precursor of elastin, mediates favorable endothelial cell interactions while having low thrombogenicity. Here we show that constructs of TE corresponding to the first 10 ("N10") and first 18 ("N18") N-terminal domains of the molecule facilitate endothelial cell attachment and proliferation equivalent to the performance of full-length TE. This N-terminal ability contrasts with the known role of the C-terminus of TE in facilitating cell attachment, particularly of fibroblasts. When immobilized on a plasma-activated coating ("PAC"), N10 and N18 retained their bioactivity and endothelial cell interactive properties, demonstrating attachment and proliferation equivalent to full-length TE. In whole blood assays, both N10 and N18 maintained the low thrombogenicity of PAC. Furthermore, these N-terminal constructs displayed far greater resistance to protease degradation by blood serine proteases kallikrein and thrombin than did full-length TE. When immobilized onto a PAC surface, these shorter constructs form a modified metal interface to establish a platform technology for biologically compatible, implantable cardiovascular devices.

[*]To whom correspondence should be addressed, School of Molecular Bioscience, University of Sydney, NSW, 2006, AUSTRALIA, Telephone: +61-2-9351 3464, Fax: +61-2 9351 5858, tony.weiss@sydney.edu.au.
[#]Equal senior authors

The authors declare no conflict of interest in this work.

1. Introduction

Metallic implants are widely used in a range of clinical applications, including prominently for cardiovascular repair. However, despite their prevalence, metallic implants interact poorly with the body, triggering inflammation, and failing to integrate with surrounding cells and tissue [1]. These problems are exacerbated in coronary stenting applications where high rates of thrombosis are observed in the absence of profound platelet suppression [2], re-endothelialization rates are suboptimal, and neointimal hyperplasia leading to restenosis is an ongoing clinical problem [3].

We have previously demonstrated the efficacy of a plasma-activated coating (PAC) to convey favorable physiological responses to metallic surfaces. PAC facilitates the covalent attachment of proteins [3, 4] by means of highly reactive radicals embedded in the plasma activated coating. Proteins, such as tropoelastin, which we have shown enhances endothelial cell attachment and proliferation, [5] are directly covalently immobilised onto PAC coated surfaces on contact with the protein solution [3]. Optimized PAC surfaces also have dramatically improved haemocompatibility compared to bare stainless steel surfaces, exhibiting minimal platelet activation and thrombosis in the presence of heparinized whole human blood [3, 6]. Recently, we demonstrated that PAC can withstand delivery *in vivo* when applied to a stent platform in an established rabbit model of stent biocompatibility [7], providing a unique opportunity to deliver a bioactive protein coating.

The promising effects of tropoelastin in the enhancement of endothelialization, suppression of smooth muscle cell infiltration and low thrombogenic potential [8] make it an excellent candidate for the modulation of vascular biocompatibility. However, we have identified that full-length TE is susceptible to degradation by abundant blood proteases kallikrein and thrombin, possibly limiting its *in vivo* lifetime [9]. We further demonstrated that a single amino acid substitution at a key protease susceptibility site significantly increased resistance to degradation. Here we aim to identify smaller functional regions of TE that support endothelial cell attachment and growth while lacking one or both of the dominant serine protease cleavage sites located in domains 10 and 26 of TE.

This study investigates endothelial cellular interactions with a panel of tropoelastin-derived constructs. Domains identified in screening that promote cell binding were translated to PAC surfaces for assessment of their capacity to support endothelial cell attachment and proliferation and investigated for haemocompatibility and susceptibility to degradation.

2. Materials and Methods

2.1 Reagents

Recombinant human tropoelastin corresponding to amino acid residues 27–724 of GenBank entry AAC98394 (gi 182020) was expressed and purified as previously described [10]. Human umbilical vein endothelial cells (HUVECs) were harvested enzymatically from umbilical cords as previously described [11]. Human coronary artery endothelial cells (HCAEC) were purchased from Cell Applications (San Diego, CA, USA). Human dermal fibroblasts (HDF; line GM3348) were obtained from Coriell Research Institute (Camden, NJ, USA). Endothelial cells from passages 2–4 and HDFs up to passage 14 were used.

2.2 Cell culture

For attachment studies, 300 cells/mm^2 were allowed to attach for 90 min in DMEM. In proliferation assays, 150 cells/mm^2 were plated for 3 and 5 days. Attachment and proliferation of cells to TE-coated wells or substrates were analyzed in comparison to tissue culture plastic alone and to wells coated with fibronectin (2 μg/mL) and 1% heat-denatured

bovine serum albumin (dBSA). At each time point, cells were washed, fixed with 3.7% formaldehyde and stained with 0.1% (w/v) crystal violet solution for 1 h at room temperature [12]. The dye was washed with distilled H_2O, solubilized with 10% (v/v) acetic acid, and the absorbance measured at 570 nm. Results were normalized to TE-coated surfaces.

2.3 Generation of plasma activated surfaces

2.3.1 Plasma ion immersion implantation (PIII)—Plasma immersion ion implantation (PIII) treatment of polystyrene (PS) surfaces was achieved using a custom-built plasma treatment system [13–15]. An inductively coupled, 100W radio-frequency discharge in high purity nitrogen at a pressure of 2×10^{-3} Torr was used for the plasma treatment. Implantation of ions extracted from the plasma was achieved by applying 20 μs, 20 kV negative bias pulses at a repetition rate of 50 Hz to the substrate holder. Samples were treated for 400 s to provide an ion fluence of 5×10^{15} ions/cm^2.

2.3.2 Plasma-activated coating (PAC)—PAC was deposited using a capacitively coupled, plasma polymerization system, configured with 100cm^2 electrodes spaced about 10 cm apart. The top electrode is rf powered while the chamber is grounded and the lower electrode left floating. The substrates, 316L stainless steel foil (SS) 25 μm thick (Brown Metals), were mounted on the lower electrode. A radio-frequency power of 50W was used to create the plasma discharge. Argon plasma cleaning, with 100 sccm Ar flow rate at a pressure of 10 Pa, was carried out for 15 min prior to the deposition of PAC. The N_2/Ar PAC layer was produced by exposing the 316L SS sheets to plasma generated in a gas mixture comprised of 50 sccm argon, 50 sccm nitrogen and 50 sccm acetylene at a pressure of 15 Pa for 1.5 min. The substrate holder was pulsed biased during the deposition time with 20 μs pulses of negative 500 V bias at 3 kHz using at RUP-6 (GBS Elektronik GmbH, Dresden, Germany) power supply.

2.4 Assessment of Covalent Binding

PIII+TE, PIII+N18 and PIII+N10 polystyrene surfaces were incubated overnight at 4°C in PBS for non-protein coated and in 50 μg/mL protein for coated PIII samples. Unbound protein was removed by aspiration and the surfaces were washed with PBS. Non-covalently bound protein was removed by SDS-washing [3]. Samples were treated with 5% (w/v) SDS for 1 h at 80°C. Following the SDS treatment, samples were washed with PBS and distilled water.

2.5 FTIR

Samples were washed with Milli-Q water to remove salt and dried prior to accumulation of spectra using a Digilab FTS7000 FTIR spectrometer fitted with an attenuated total reflection (ATR) accessory with a trapezium germanium crystal at incidence angle of 45°. To obtain sufficient signal/noise ratio and resolution of spectral bands, 500 scans with a resolution of 1 cm^{-1} were taken. Difference spectra were used to detect changes associated with the presence of TE. Spectral analysis and subtraction was performed using GRAMS software.

The amount of the attached protein was calculated from the absorbances of amide A (3300 cm^{-1}), I (1650 cm^{-1}) and II (1540 cm^{-1}) peaks corresponding to protein backbone vibrations. The intensity of the PS vibration peak at 1452 cm^{-1} was used as an internal standard for normalization. The extinction coefficients for amide lines and the procedure used to calculate the amount of protein were described previously [16].

2.6 Thrombogenicity assessment

Whole blood was obtained from healthy, non-smoking male volunteers, with informed consent in accordance with the Declaration of Helsinki who had not consumed aspirin 2 weeks prior to donation. Approval for this work was granted by The University of Sydney, Human Research Ethics Committee (protocol 05-2009/11668). Experiments were conducted in triplicate with blood from different donors.

2.6.1 Static whole blood adhesion—Samples of 316L SS, PAC, PAC + N10 and PAC + N18 surfaces were incubated overnight at 4°C in PBS for non-protein treated and 50 μg/mL of each protein construct for protein-coated samples. Surfaces were rocked with heparinized whole blood (0.5 U/ml) for up to 60 min at 37°C as in [6].

2.6.2 Modified Chandler loop—Evaluation of surface thrombogenicity was performed using a modified Chandler loop as described previously [6]. Pre-weighed surfaces were inserted into loops constructed of Tygon S-50-HL tubing (SDR, Australia). Loops were filled with heparinized human whole blood (0.5 U/mL), enclosed with 1 cm silicon connectors and rotated at 34 rpm at 37°C to simulate mean coronary artery flow rate (85 mL/min) over a time course. Surfaces and thrombi were removed at each time point, imaged using a Nikon 5100D camera and weighed.

2.7 Scanning electron microscopy (SEM)

Samples were fixed in 2.5% glutaraldehyde, post-fixed with 1% (v/v) osmium tetroxide, and dehydrated in ascending grades of ethanol before drying with hexamethyldisilazane. The samples were sputter coated with 20 nm gold and imaged with a Philips XL 30 CP scanning electron microscope.

2.8 Protease susceptibility

2.8.1 Degradation study—Samples were incubated with 10 μM human thrombin (Novagen) or 4.5 μM kallikrein (Sigma-Aldrich) [8] in a humidified incubator at 37°C. At each time point, proteases were inactivated with the addition of 1 mM PMSF.

2.8.2 SDS-PAGE—Samples were boiled at 95°C for 10 min, debris pelleted (10 000 × g, 1 min) and run (200V, 40 min) on a 4–20% Tris-Glycine gel (Bio-Rad). Gels were immediately fixed for 30 min and stained with blue-silver stain for 1 h. Destained gels were imaged on a Li-Cor Odyssey and quantified using ImageJ.

2.9 Statistical analysis

Data are expressed as mean ± SEM. Groups were compared by a 1-way analysis of variance (ANOVA) with post-hoc analyses for pairwise comparisons (Bonferroni post-test); statistical significance was inferred at a 2-sided value of $p<0.05$ using GraphPad Prism v. 5.00 for Mac.

3. Results

3.1 Constructs of TE

A panel of previously characterized tropoelastin-derived constructs (Fig. 1) was produced and assessed following RP-HPLC purification by mass spectrometry and SDS-PAGE analysis. All constructs displayed expected identities and were free of detectable degradation products.

3.2 Cellular attachment to the TE C-terminus

The importance of the C-terminal region of tropoelastin, specifically the terminal RKRK sequence in mediating fibroblast binding has been shown [12]. Examination of ΔRKRK, domain 36 only and 36S confirmed fibroblast behavior with the current constructs (Fig. 2A). We then assessed endothelial cell attachment to tropoelastin-derived constructs for both human umbilical vein endothelial cells (HUVECs) and human coronary artery endothelial cells (HCAECs). In contrast to fibroblasts, endothelial cell attachment to ΔRKRK did not significantly differ from TE, while binding to domain 36 and 36S constructs were essentially indistinguishable from background (Fig. 2B, C). This marked difference in the attachment behavior of fibroblasts and endothelial cells led us to investigate the endothelial attachment potential of other regions of TE.

3.3 Upstream TE regions and EC binding

Constructs based on the TE sequence containing the N-terminus, but not the C-terminus (N25 and N18), and lacking either end (17–27) were examined for their capacity to facilitate the attachment of endothelial cells. N25 and 17–27 showed significantly lower EC attachment (48±1.2% and 44±1.4%, $p<0.01$), while N18 displayed attachment equivalent to that of the full-length TE control (Fig. 3A, B). Further examination of the role of the TE N-terminal arm using a shorter construct that corresponded to the first 10 domains of TE (N10), showed equivalent binding to TE and N18 (Fig. 3C, D). Our cell attachment data were similar for HUVECs and HCAECs.

3.4 EC proliferation on N-terminal constructs

As EC attachment was strong, we then assessed proliferation on TE, N18 and N10 coated surfaces (Fig. 4A). Following a 3-day incubation, cell numbers on TE, N18 and N10 were equivalent and all significantly greater than dBSA-coated control wells ($p<0.001$). The FN positive control was significantly higher than all TE constructs at day 3 ($p<0.001$). Cell numbers on TE coated wells increased 2.5±0.2 fold between days 3 and 5, demonstrating strong EC proliferation on this surface. By day 5, TE, N18, N10 and FN all showed equivalent cell numbers, and all were significantly greater than dBSA ($p<0.001$). Characteristic endothelial cell phenotypes were maintained on all TE constructs and FN coated wells, as demonstrated by representative images (Fig. 4B). Additional experiments observing HCAEC proliferation yielded equivalent results (data not shown).

3.5 Covalent immobilization

Spectra of PIII plasma surfaces after incubation with TE, N18 and N10 (Fig. 5A) contained characteristic peaks associated with the internal protein vibrations. For comparison, the peak intensities were normalized to the intensity of the polystyrene peak at 1452 cm^{-1}.

The relative intensities of characteristic amide A, I and II FTIR peaks for TE, N18 and N10 were compared before and after washing with detergent (Fig. 5B). Initial differences in protein amounts prior to washing can be attributed to a blend of variously amassed non-covalently and covalently bound protein. After detergent washing, surfaces displayed only covalently attached protein, all at comparable levels. PIII polystyrene and PAC deposited on stainless steel have similar chemistry and TE binding mechanisms [3, 4]; thus the covalent binding observed on polystyrene was tested on PAC.

3.6 ECs and immobilized TE constructs

Consistent with observations on tissue culture plastic, endothelial cell attachment was equivalent for TE, N18 and N10, following immobilization on PAC. All constructs attached more ECs than did the dBSA control (Fig. 5C). Similarly, the proliferative trend for ECs

was mirrored for immobilized constructs (Fig. 5D). PAC alone and SS controls demonstrated cell increases between days 3 and 5, although these were small compared to the large increases seen for TE-, N18- and N10-coated surfaces. Here too each of the constructs showed efficacy equivalent to the full-length TE (Fig. 5D).

3.7 Blood compatibility

The relative thrombogenicity of TE, N18 and N10 bound to PAC was studied using a whole blood adhesion assay (Fig. 6A). Untreated 316L SS surfaces bound and activated blood components after 15 min, including fibrin, red blood cells and platelets. By 30 min, this effect was amplified as surfaces were covered with clotted blood. PAC alone and PAC coated with TE or N18 displayed no discernible binding of blood factors over the time course. Under flow conditions, stainless steel induced substantial (60±10 mg) thrombus formation (Fig. 5B). In contrast, the thrombogenicity of PAC alone reduced significantly ~25 fold to 2.0±0.6 mg ($p<0.001$) and PAC+N18 (0.7±0.3 mg) and PAC+N10 (1.1±0.3 mg) retained this improvement.

3.8 Protease susceptibility

TE, N18 and N10 were subjected to supra-physiological levels of two abundant blood serine proteases: thrombin and kallikrein. During 1 h and 6 h incubations, N18 and N10 demonstrated higher resistance to proteolysis than did TE. The addition of thrombin reduced intact protein levels to 19.4±1.3% (TE), 79.3±2.7% (N18) and 92.2±2.0% (N10) after 1 h; and 3.2±2.0% (TE), 47.9±2.2% (N18), 71.9±3.6% (N10) at 6 h. Similarly, kallikrein incubations decreased intact protein levels after 1 h to 56.5±2.8% (TE), 77.2±3.4% (N18) and 89.2±2.8% (N10); and 22.8±11% (TE), 72.9±1.7% (N18) and 87.2±4.1% (N10) at 6 h.

4. Discussion

Vascular biomaterial applications have benefited from tropoelastin's vascular performance including low thrombogenicity coupled with its ability to inhibit smooth muscle cells and enhance endothelialization [17]. To increase the efficacy of TE in these applications we aimed to identify key regions within the protein responsible for these properties, particularly focusing on endothelial cell interactions and protease resistance while having low thrombogenicity.

As EC binding to tropoelastin had not been fully elucidated, we utilized a well characterized binding interaction between human dermal fibroblasts and tropoelastin at the extreme C-terminal RKRK sequence as part of the region encoded by exon 36 [12, 18]. In direct contrast to the fibroblast interaction, ECs showed binding to ΔRKRK that was equivalent to that of the full-length TE, and no binding to domain 36 or 36S. These findings collectively discounted dependence on this region. We then turned to upstream constructs of TE and through the use of various constructs identified full binding to N18. Differences between these overlapping constructs fit with previously published work showing that N18 adopts an altered conformation relative to N25 [19] and benefits from an appreciation of structural presentation of the molecule [20].

We chose to focus on strong binding to the N-terminus, and on this basis found that N10 and N18 mediate the same level of EC attachment as does full-length TE. These results point to the biomaterials potential of EC-attraction that would be mediated by these N-terminally-derived parts of TE. The production process for N18 generated significantly higher yields than for N10, prompting us to continue a parallel investigation of these constructs and gain a full understanding of their relative efficacy.

To study the covalent binding of N10 and N18, we used a well-characterized PIII treated polystyrene system [21] which facilitated FTIR monitoring of protein peaks before and after SDS washing, and confirmed covalent bonding between protein and substrate through a free radical driven mechanism for PIII and plasma polymerized surfaces [22]. Following N10 and N18 immobilization on PAC, each maintained EC attachment and proliferation found on tissue culture plastic, confirming that the biological function of the constructs was retained on PAC.

Surface thrombogenicity of the immobilized constructs was assessed using established whole blood assays in rocking and flow conditions [6]. After 30 min of rocking in heparinized whole blood, PAC showed no detectable adhesion of blood components. In contrast, untreated 316L SS surfaces bound and activated blood components after 15 min and included fibrin, red blood cells and platelets. By 30 min SS surfaces showed signs of advanced clot formation. The covalent addition of N10 and N18 constructs on PAC maintained its non-thrombogenic performance, as evidenced by the absence of clotting factors on these surfaces at 30 min. This effect is consistent with previous data on PAC+TE [6]. Following a 30 min incubation under flow, uncoated SS showed significant thrombus formation at rates over 6 fold above PAC and PAC + protein coated conditions. No differences were observed between PAC, PAC+N10 and PAC+N18 surfaces, i.e. the tropoelastin-based constructs maintained the non-thrombogenic properties of PAC when exposed to flowing whole blood.

On the basis of the twin criteria of EC interactions and blood compatibility, N10 and N18 performed as well as TE. However, TE is susceptible to proteolytic cleavage by blood serine proteases, particularly kallikrein and thrombin, potentially reducing its application in such a protease-rich environment *in vivo* [8, 23]. We have previously shown that changing a specific amino acid at a protease recognition site (R515A) increases TE's protease resistance by up to 20% [9]. Here we showed that truncated N10 and N18, which lack both or one of the known susceptibility sites respectively, show further resistance to degradation relative to full-length TE. On this basis N10, the shortest segment we studied, had the highest resistance; it remained substantially intact even after substantial supra-physiological protease exposure. We propose that this improved resistance *in vitro* would usefully extend the *in vivo* lifetime of either construct when covalently immobilized on implanted PAC surfaces. Further investigations to uncover the mechanisms of cell interaction with these N-terminal regions would be useful in building our understanding of this process and may ultimately allow the production of still shorter constructs that reflect the desired aspects of the activity of the full-length protein.

Conclusions

The N-terminus of tropoelastin helps to drive endothelial cell attachment and proliferation, whose response is surprisingly diminished in these cells for the C-terminus. PAC-coated constructs that utilize N10 and N18 have vascular utility because they maintain their bioactivity when immobilized on plasma-treated surfaces and preserve the low thrombogenicity of these surfaces. For *in vivo* applications, these N-terminal constructs provide an advantage over the full-length tropoelastin due to their increased resistance to protease degradation.

Acknowledgments

We acknowledge funding from the Australian Research Council (M.M.M.B and A.S.W.), Australian Defense Health Foundation (A.S.W.), National Health and Medical Research Council (APP1033079 and APP1039072; A.S.W., M.M.M.B and M.K.C.N.) and National Institutes of Health (EB014283 and HL107503; A.S.W.). A.S.W. is

the Scientific Founder of Elastagen Pty Ltd. The authors also acknowledge the facilities as well as scientific and technical assistance at the Australian Centre for Microscopy and Microanalysis.

References

1. Mani G, Feldman MD, Patel D, Agrawal CM. Coronary stents: a materials perspective. Biomaterials. 2007; 28:1689–710. [PubMed: 17188349]
2. Serruys P, Strauss B, Beatt K, Bertrand M, Puel J, Rickards A, et al. Angiographic follow-up after placement of a self-expanding coronary-artery stent. N Engl J Med. 1991; 324:13–7. [PubMed: 1984159]
3. Bilek MM, Bax DV, Kondyurin A, Yin Y, Nosworthy NJ, Fisher K, et al. Free radical functionalization of surfaces to prevent adverse responses to biomedical devices. Proc Natl Acad Sci U S A. 2011; 108:14405–10. [PubMed: 21844370]
4. Bilek MM, McKenzie DR. Plasma modified surfaces for covalent immobilization of functional biomolecules in the absence of chemical linkers: towards better biosensors and a new generation of medical implants. Biophys Rev. 2010; 2:55–65.
5. Yin Y, Wise SG, Nosworthy NJ, Waterhouse A, Bax DV, Youssef H, et al. Covalent immobilisation of tropoelastin on a plasma deposited interface for enhancement of endothelialisation on metal surfaces. Biomaterials. 2009; 30:1675–81. [PubMed: 19157535]
6. Waterhouse A, Yin YB, Wise SG, Bax DV, McKenzie DR, Bilek MMM, et al. The immobilization of recombinant human tropoelastin on metals using a plasma-activated coating to improve the biocompatibility of coronary stents. Biomaterials. 2010; 31:8332–40. [PubMed: 20708259]
7. Waterhouse A, Wise SG, Yin Y, Wu B, James B, Zreiqat H, et al. In vivo biocompatibility of a plasma-activated, coronary stent coating. Biomaterials. 2012; 33:7984–92. [PubMed: 22889486]
8. Waterhouse A, Wise SG, Ng MK, Weiss AS. Elastin as a nonthrombogenic biomaterial. Tissue Eng Part B Rev. 2011; 17:93–9. [PubMed: 21166482]
9. Waterhouse A, Bax DV, Wise SG, Yin Y, Dunn LL, Yeo GC, et al. Stability of a therapeutic layer of immobilized recombinant human tropoelastin on a plasma-activated coated surface. Pharm Res. 2011; 28:1415–21. [PubMed: 21103913]
10. Wu W, Vrhovski B, Weiss A. Glycosaminoglycans mediate the coacervation of human tropoelastin through dominant charge interactions involving lysine side chains. J Biol Chem. 1999; 274:21719–24. [PubMed: 10419484]
11. Ng M, Nakhla S, Baoutina A, Jessup W, Handelsman D, Celermajer D. Dehydroepiandrosterone, an adrenalandrogen, increases human foam cell formation: a potentially pro-atherogenic effect. J Am Coll Cardiol. 2003; 42:1967–74. [PubMed: 14662261]
12. Bax D, Rodgers U, Bilek M, Weiss A. Cell adhesion to tropoelastin is mediated via the c-terminal grkrk motif and integrin $\alpha_V\beta_3$. J Biol Chem. 2009; 284:28616–23. [PubMed: 19617625]
13. Bax DV, Wang Y, Li Z, Maitz PK, McKenzie DR, Bilek MM, et al. Binding of the cell adhesive protein tropoelastin to PTFE through plasma immersion ion implantation treatment. Biomaterials. 2011; 32:5100–11. [PubMed: 21527206]
14. MacDonald C, Morrow R, Weiss AS, Bilek MM. Covalent attachment of functional protein to polymer surfaces: a novel one-step dry process. J R Soc Interface. 2008; 5:663–9. [PubMed: 18285286]
15. Gan BK, Nosworthy NJ, McKenzie DR, Dos Remedios CG, Bilek MM. Plasma immersion ion implantation treatment of polyethylene for enhanced binding of active horseradish peroxidase. J Biomed Mater Res A. 2008; 85:605–10. [PubMed: 17806119]
16. Kondyurin AV, Naseri P, Tilley JMR, Nosworthy NJ, Bilek MMM, McKenzie DR. Mechanisms for Covalent Immobilization of Horseradish Peroxidase on Ion-Beam-Treated Polyethylene. Scientifica. 2012; 2012:1–28.
17. Mithieux SM, Wise SG, Weiss AS. Tropoelastin - A multifaceted naturally smart material. Adv Drug Deliv Rev. 2013; 65:421–8. [PubMed: 22784558]
18. Rodgers UR, Weiss AS. Integrin alpha v beta 3 binds a unique non-RGD site near the C-terminus of human tropoelastin. Biochimie. 2004; 86:173–8. [PubMed: 15134831]

19. Baldock C, Oberhauser AF, Ma L, Lammie D, Siegler V, Mithieux S, et al. Shape of tropoelastin, the highly extensible protein that controls human tissue elasticity. Proc Natl Acad Sci U S A. 2011; 108:4322–7. [PubMed: 21368178]

20. Yeo GC, Baldock C, Tuukkanen A, Roessle M, Dyksterhuis LB, Wise SG, et al. Tropoelastin bridge region positions the cell-interactive C terminus and contributes to elastic fiber assembly. Proc Natl Acad Sci U S A. 2012; 109:2878–83. [PubMed: 22328151]

21. Bax DV, McKenzie DR, Weiss AS, Bilek MM. Linker-free covalent attachment of the extracellular matrix protein tropoelastin to a polymer surface for directed cell spreading. Acta Biomater. 2009; 5:3371–81. [PubMed: 19463976]

22. Yin YB, Fisher K, Nosworthy NJ, Bax D, Rubanov S, Gong B, et al. covalently bound biomimetic layers on plasma polymers with graded metallic interfaces for in vivo implants. Plasma process and polym. 2009; 6:658–66.

23. Jensen SA, Vrhovski B, Weiss AS. Domain 26 of tropoelastin plays a dominant role in association by coacervation. J Biol Chem. 2000; 275:28449–54. [PubMed: 10862774]

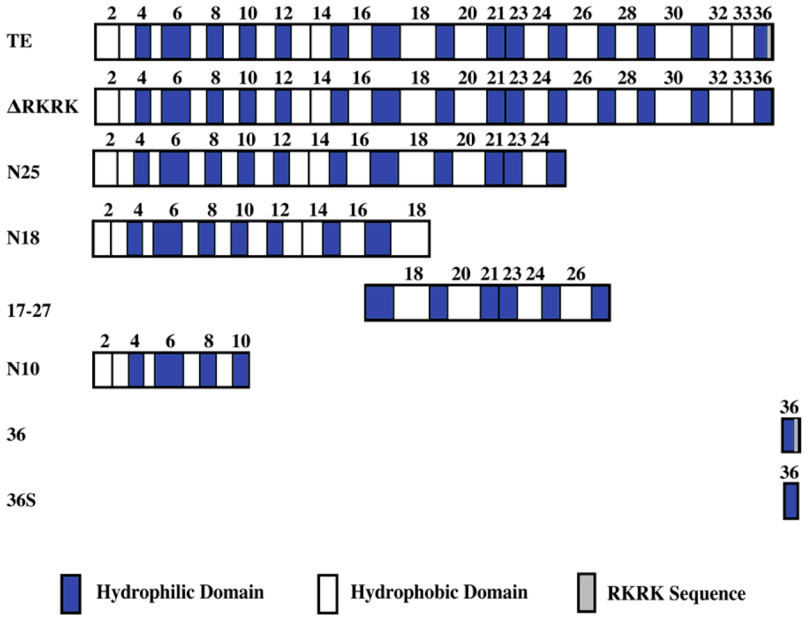

Figure 1.
Panel of tropoelastin-based constructs. Key domain features are indicated.

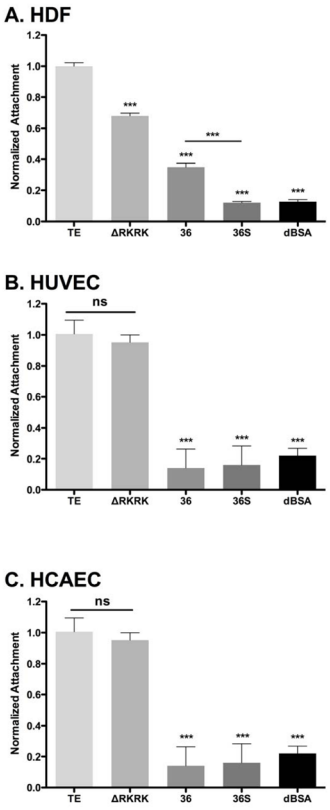

Figure 2.

Attachment of (A) human dermal fibroblasts (B) HUVEC and (C) HCAEC to C-terminus-focused tropoelastin constructs. Tissue culture surfaces were coated with tropoelastin (TE), ΔRKRK, peptide 36 (36) or peptide 36 short (36S) overnight. Cell attachment was quantified with crystal violet staining 90 min post-seeding and normalized to tropoelastin-coated surfaces. Significance is relative to TE.

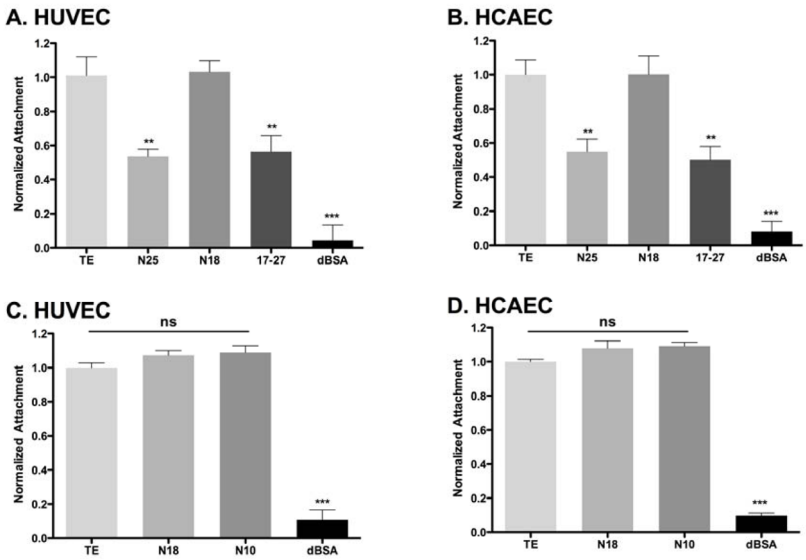

Figure 3.

Endothelial cell attachment to broad regions of (A, B) tropoelastin and (C, D) N-terminal constructs. HUVECs and HCAECs displayed reduced attachment to the N25 and 17–27 constructs, however the N10 and N18 restored cell attachment to equivalent levels of TE. Significance is relative to TE.

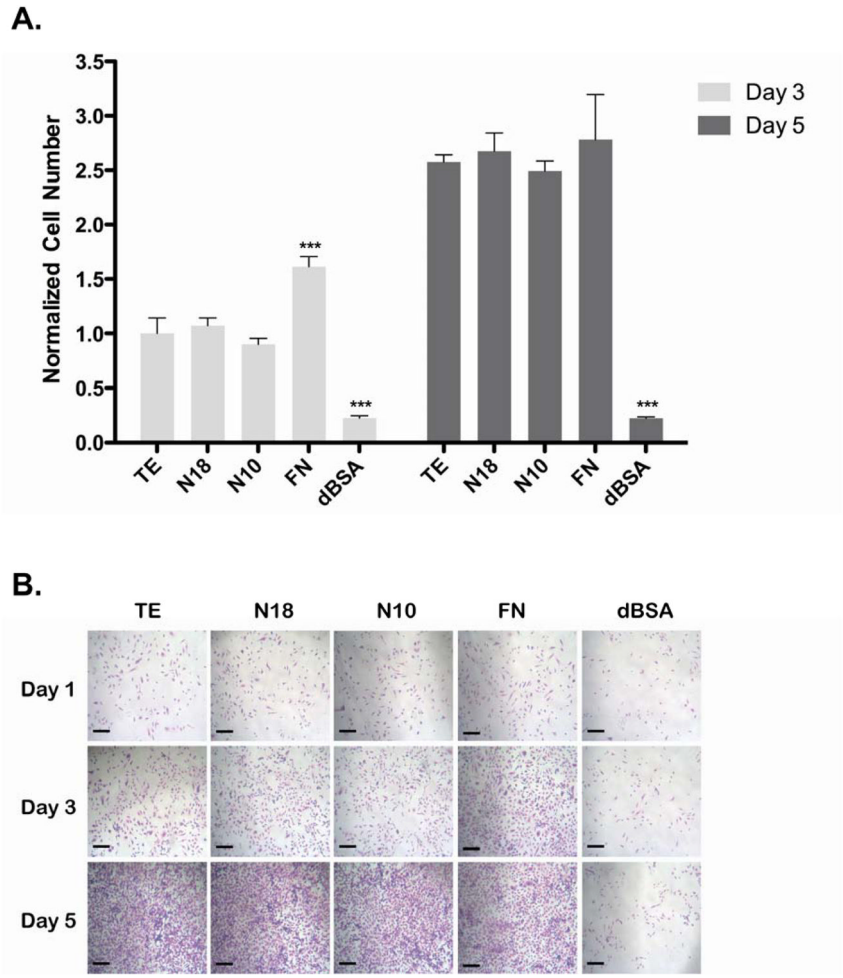

Figure 4.

HUVEC proliferation on coated surfaces. Cells grew over 3 and 5 days, with a media change on day 3. Cell numbers were quantified by (A) crystal violet staining and (B) visualized by light microscopy. Scale bars are 100 μm. Significance at each time point is relative to TE.

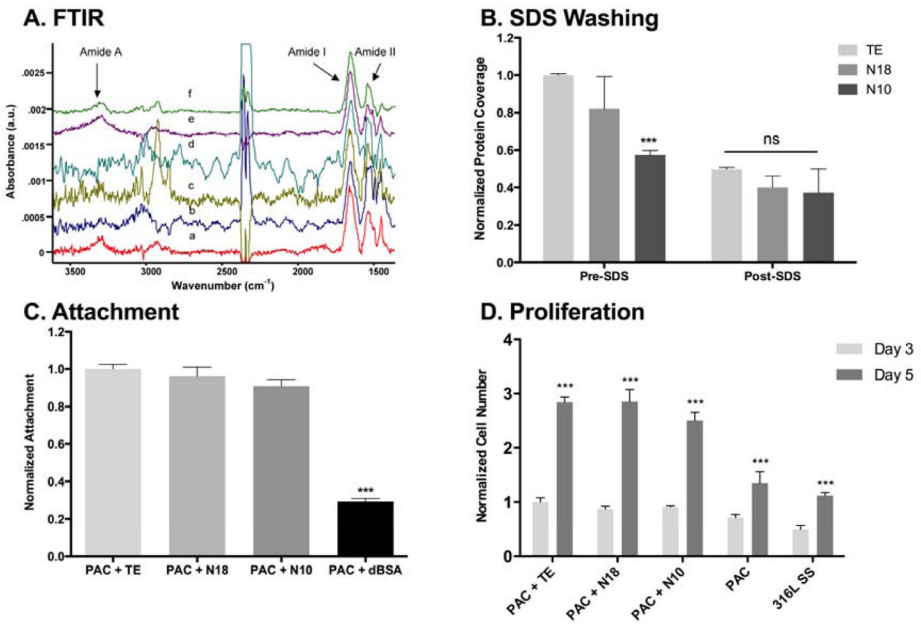

Figure 5.

Characterization of immobilized protein and cellular response on plasma-activated surfaces. (A, B) FTIR spectroscopy of immobilized constructs (C, D) HUVEC attachment and proliferation on immobilized proteins assessed using crystal violet staining. Significance is relative to (C) TE and (D) the respective value on day 3.

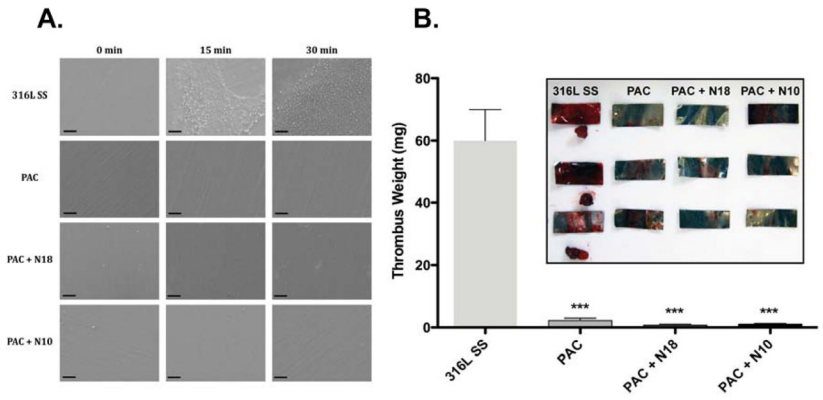

Figure 6.

Thrombogenicity assessment of coated surfaces. Surfaces were exposed to whole blood under rocking (A) or flow conditions (B). Static conditions were imaged by SEM. Thrombi present under flow conditions were weighed (B) and (inset) imaged.

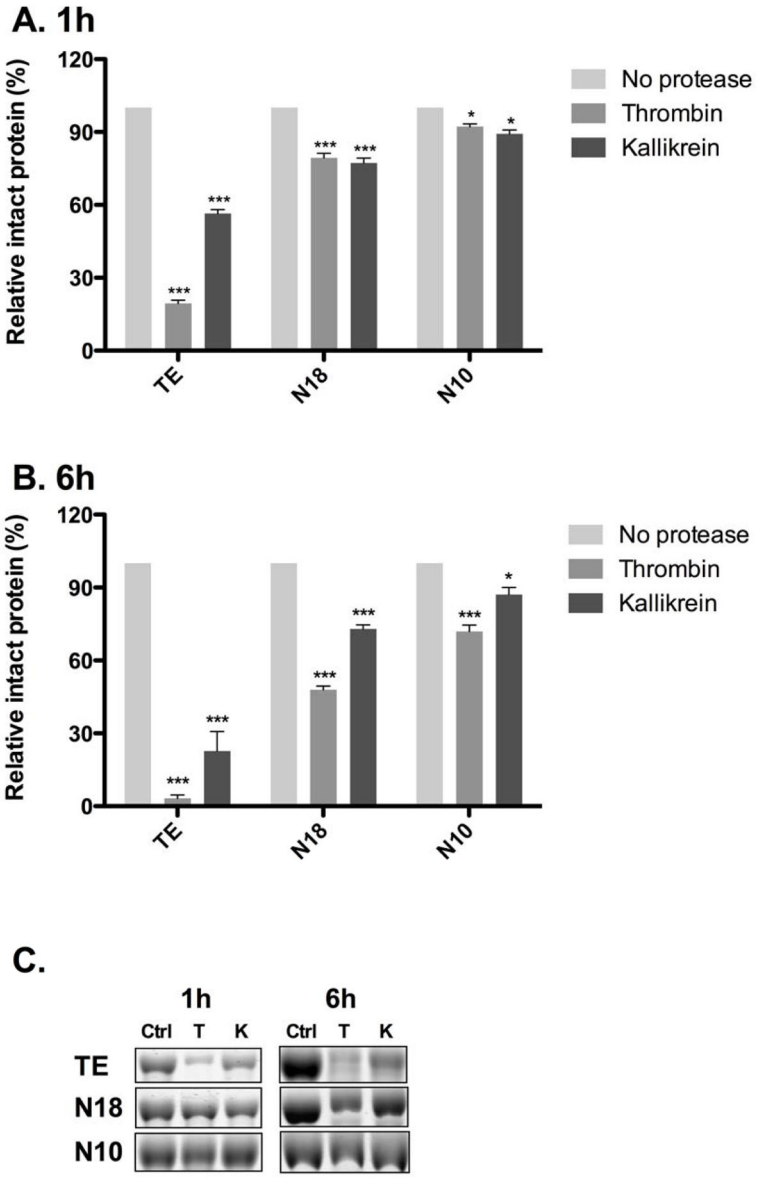

Figure 7.

Evaluation of construct susceptibility to proteolytic degradation. Retained protein following exposure to proteases at 1 h (A, C) and 6 h (B, C) was quantified by measuring optical density. Significance is relative to the protease-free control for each construct.